THE JOURNAL OF BIOLOGICAL CHEMISTRY Vol. 276, No. 49, Issue of December 7, pp. 45516–45521, 2001
Printed in U.S.A.

Tyrosine Iminoxyl Radical Formation from Tyrosyl Radical/Nitric Oxide and Nitrosotyrosine*

Received for publication, July 19, 2001
Published, JBC Papers in Press, September 10, 2001, DOI 10.1074/jbc.M106835200

Bradley E. Sturgeon‡, Richard E. Glover, Yeong-Renn Chen, Leo T. Burka, and Ronald P. Mason

From the Laboratory of Pharmacology and Chemistry, NIEHS, National Institutes of Health, Research Triangle Park, North Carolina 27709

The quenching of the $Y_D^{\cdot}$ tyrosyl radical in photosystem II by nitric oxide was reported to result from the formation of a weak tyrosyl radical-nitric oxide complex (Petrouleas, V., and Diner, B. A. (1990) *Biochim. Biophys. Acta* 1015, 131–140). This radical/radical reaction is expected to generate an electron spin resonance (ESR)-silent 3-nitrosocyclohexadienone species that can reversibly regenerate the tyrosyl radical and nitric oxide or undergo rearrangement to form 3-nitrosotyrosine. It has been proposed that 3-nitrosotyrosine can be oxidized by one electron to form the tyrosine iminoxyl radical (>C=N-O$^{\cdot}$). This proposal was put forth as a result of ESR detection of the iminoxyl radical intermediate when photosystem II was exposed to nitric oxide (Sanakis, Y., Goussias, C., Mason, R. P., and Petrouleas, V. (1997) *Biochemistry* 36, 1411–1417). A similar iminoxyl radical was detected in prostaglandin H synthase-2 (Gunther, M. R., Hsi, L. C., Curtis, J. F., Gierse, J. K., Marnett, L. J., Eling, T. E., and Mason, R. P. (1997) *J. Biol. Chem.*, 272, 17086–17090). Although the iminoxyl radicals detected in the photosystem II and prostaglandin H synthase-2 systems strongly suggest a mechanism involving 3-nitrosotyrosine, the iminoxyl radical ESR spectrum was not unequivocally identified as originating from tyrosine. We report here the detection of the non-protein L-tyrosine iminoxyl radical generated by two methods: 1) peroxidase oxidation of synthetic 3-nitroso-*N*-acetyl-L-tyrosine and 2) peroxidase oxidation of free L-tyrosine in the presence of nitric oxide. A newly developed ESR technique that uses immobilized enzyme was used to perform the ESR experiments. Analysis of the high resolution ESR spectrum of the tyrosine iminoxyl radical generated from free tyrosine and nitric oxide reveals a 28.4-G isotropic nitrogen hyperfine coupling and a 2.2-G proton hyperfine coupling assigned to the proton originally *ortho* to the phenoxyl oxygen.

Protein-derived radicals play an important role in enzymatic catalysis (1). The tyrosyl radical has been identified in a number of enzyme systems including photosystem II (2, 3), ribonucleotide reductase (4, 5), prostaglandin H synthase (6), DNA photolyase (7, 8), and bovine liver catalase (9). Modified tyrosyl radicals have been observed in galactose oxidase (10, 11) and cytochrome *c* oxidase (12). The reaction of a tyrosyl radical cofactor with nitric oxide has been shown to inhibit enzyme activity. When photosystem II is exposed to NO, the stable tyrosyl radical cofactor $Y_D^{\cdot}$ is reversibly quenched (13). In addition, NO reversibly quenches the redox-active $Y_Z^{\cdot}$ in manganese-depleted photosystem II and the S3 state (an exchange-coupled complex involving $Y_Z^{\cdot}$) in acetate-treated photosystem II (14). When ribonucleotide reductase is exposed to NO, enzymatic activity is diminished; in addition the tyrosyl radical cofactor that resides on the R2 subunit is reversibly quenched (15–17). These studies with photosystem II and ribonucleotide reductase provide important insights into the reactivity of the tyrosyl radical and NO but provide little information regarding the nature of the tyrosyl radical/NO interaction.

Exposure of photosystem II to NO followed by illumination at 200 K results in the quenching of the tyrosyl radical and the formation of an additional radical species that was assigned by ESR[1] as the tyrosine iminoxyl radical (>C=N-O$^{\cdot}$) based on the large nitrogen hyperfine-coupling constant (A_{iso} = 29.3 G) (18). When prostaglandin H synthase-2 is exposed to NO, the tyrosyl radical associated with enzymatic turnover is eliminated, and an additional radical species, similar to the one seen during the NO exposure/illumination in photosystem II, is detected. This radical is also assigned to the tyrosine iminoxyl radical (19, 20). The observation of the tyrosine iminoxyl radical species in photosystem II and prostaglandin H synthase-2 prompted the proposal of Scheme 1.

The reaction between tyrosyl radical (Scheme 1, *A*) and NO is near diffusion limited ($1–2 \times 10^9$ M^{-1} s^{-1}) (21); a major product is expected to be the ESR-silent 3-nitrosocyclohexadienone species (Scheme 1, *B*). A prototropic rearrangement of *B* results in the formation of 3-nitrosotyrosine (Scheme 1, *C*), which is in equilibrium with its oxime tautomer, *C′*. The one-electron oxidation of *C* or *C′* results in the formation of the tyrosine iminoxyl radical (Scheme 1, *D*). The source of the oxidative equivalent needed to convert *C*/*C′* to *D* in the enzyme systems is not clear, although it has been proposed that *C*/*C′* is oxidized by the light-driven reactions in photosystem II (18) and by the peroxidase activity in prostaglandin H synthase-2 (19). The one-electron oxidation of the iminoxyl radical has been proposed to form 3-nitrotyrosine (19).

We have continued the investigation of the tyrosyl radical and NO chemistry depicted in Scheme 1. Although the ESR spectra of the iminoxyl radicals detected in photosystem II and

* The costs of publication of this article were defrayed in part by the payment of page charges. This article must therefore be hereby marked "*advertisement*" in accordance with 18 U.S.C. Section 1734 solely to indicate this fact.

‡ To whom correspondence should be addressed. North Carolina School of Science and Mathematics, 1219 Broad St., Durham, NC 27705. Tel.: 919-416-2774; Fax: 919-416-2890. E-mail: sturgeon@ncssm.edu.

[1] The abbreviations used are: ESR, electron spin resonance; MOPS, 3-(*N*-morpholino)propanesulfonic acid; DTPA, diethylenetriaminepentaacetic acid; HRP, horseradish peroxidase; HRP_i, immobilized HRP; TEMPO, 4-hydroxy-2,2,6,6-tetramethylpiperidine-1-oxyl; HRP-I, horseradish peroxidase-compound I; HRP-II, horseradish peroxidase-compound II.

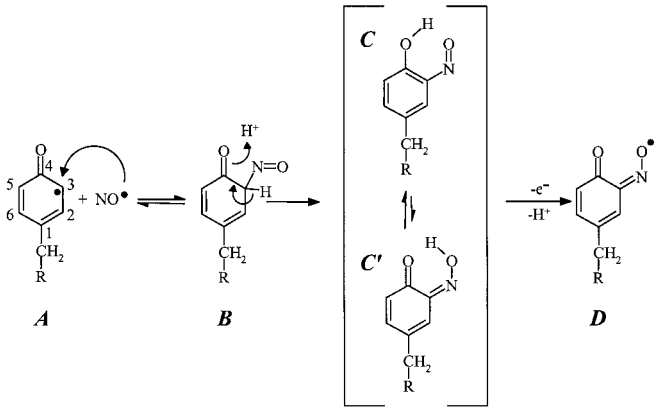

SCHEME 1.

prostaglandin H synthase-2 strongly support the chemistry in Scheme 1, the ESR spectra are from polycrystalline samples with broad ESR linewidths and display a single hyperfine coupling from the iminoxyl nitrogen. The nitrogen hyperfine parameters are identified as originating from the nitrogen of NO. However, no tyrosine-derived nuclei are identified; thus the iminoxyl radical was not unequivocally identified as originating from tyrosine. In this study, we report the ESR detection of the protein-free L-tyrosine iminoxyl radical generated by two methods: 1) peroxidase oxidation of synthetic 3-nitroso-*N*-acetyl-L-tyrosine and 2) peroxidase oxidation of free L-tyrosine in the presence of NO. The immobilized (77 K) ESR spectrum of the *N*-acetyl-L-tyrosine iminoxyl radical was nearly identical to the iminoxyl radical detected in photosystem II and prostaglandin H synthase-2. The reactivity of the tyrosine iminoxyl radical with the antioxidant ascorbate was also investigated.

EXPERIMENTAL PROCEDURES

Materials—L-Tyrosine, *N*-acetyl-L-tyrosine, ascorbic acid, sodium nitrite, MOPS, diethylenetriaminepentaacetic acid (DTPA), and glycine ethyl ester were purchased from Sigma and were used as received. Hydroxylamine hydrochloride, sodium amminepentacyanoferrate (II) hydrate, and *N*-acetyl-L-tyrosine used in the synthesis of 3-nitroso-*N*-acetyl-L-tyrosine were purchased from Aldrich. Horseradish peroxidase (EC 1.11.1.7) type VI-A was purchased from Sigma. Hydrogen peroxide was purchased from Fischer Scientific (Pittsburgh, PA); concentrations were verified using the UV absorbance at 240 nm (ϵ = 43.6 cm^{-1} M^{-1}). Tyrosine isotopes, L-4-hydroxyphenyl-3,5-d_2-alanine, referred to in this study as 3,5-d_2-L-tyrosine, and L-4-hydroxyphenyl-2,6-d_2-alanine, referred in this study as 2,6-d_2-L-tyrosine, were purchased from Isotec Inc. (Miamisburg, OH) and used as received. NO (99% minimum, CP grade) was purchased from National Specialty Gases (Durham, NC). The preparation of NO solutions was carried out in a certified fume hood. Spent NO solutions were allowed to air oxidize within the fume hood or reacted with a molar excess solution of potassium permanganate prior to disposal (22). Affi-Gel 10 and Chelex-100 were purchased from Bio-Rad Laboratories, Inc. (Hercules, CA). Enzyme dialysis was done using Slide-A-Lyzer cassettes, and M_r 10,000 cutoff was purchased from Pierce. Sodium phosphate monobasic monohydrate and sodium phosphate dibasic heptahydrate were purchased from Mallinckrodt (Paris, KY). All buffers were made fresh daily from a 10-fold concentrate that underwent a 24-h Chelex-100 treatment; DTPA was added to the buffer concentrate after removal of Chelex-100. Final buffer concentrations (50 mM phosphate and 50 μM DTPA) were obtained by dilution with HPLC water followed by pH adjustment to 7.4.

Preparation of Synthetic 3-Nitroso-N-acetyl-L-tyrosine—The synthesis of 3-nitroso-*N*-acetyl-L-tyrosine was adapted from a synthesis of nitrosophenols by Maruyama *et al.* (23). *N*-Acetyl-L-tyrosine (1 G, 4.5 mmol) was dissolved in 20 ml of water; 1.6 G (23 mmol) of hydroxylamine hydrochloride and 0.82 G (3 mmol) of sodium amminepentacyanoferrate (II) hydrate were added while stirring. Stirring was continued while 2 ml (18 mmol) of 30% H_2O_2 was added dropwise over a period of 5–10 min. The mixture was stirred for 1 h, and the product was isolated by reversed phase (C-18) low pressure chromatography. A step gradient (100 ml portions of 0.1% trifluoroacetic acid in H_2O, MeOH in 5% steps) was used to elute the product from the column. The product eluted in 15% MeOH. The product was not stable, and attempts to further purify it were unsuccessful. ^{1}H NMR (CD_3OD) d 7.33 (d, J = 9 Hz, 4-CH), 6.88 (br s, 2-CH), 6.83 (dd, J = 9 and 1.5 Hz), 4.73 (dd, J = 5 and 9 Hz, a-CH), 3.18 (dd, J = 5 and 14 Hz, b-CH), 2.93 (dd, J = 9 and 14 Hz, b-CH) and 1.92 (s, $COCH_3$); MS (TOF, ES^+) 253 (M+H). Experiments using 3-nitroso-*N*-acetyl-L-tyrosine were done immediately following the preparation.

Preparation of Immobilized Enzyme for ESR Experiments—Horseradish peroxidase (HRP) type VI-A was dialyzed against a 0.1 M MOPS buffer (pH 7.5) for 6 h with one change of buffer. HRP was recovered from the dialysis cassette and coupled to an activated agarose gel bead support (Affi-Gel 10) via the primary amino group as outlined in the product literature. A subscript "i" will be used to denote the immobilized enzyme (*i.e.* immobilized horseradish peroxidase = HRP_i). The use of immobilized enzymes for the direct ESR detection of enzyme-generated radicals was developed and evaluated in our laboratory.[2] The HRP_i (~100 μl) was transferred into a 10-mm quartz flat cell and then washed with buffer. A small glass wool plug in the outlet side of the flat cell prevented the loss of HRP_i during flow conditions. The activity of the HRP_i was based on the milligrams of enzyme bound per bed volume of agarose gel bead support. The concentration of the enzyme solution prior to agarose bead exposure was compared with the concentration after exposure to determine the milligrams of enzyme immobilized. Free enzyme concentration was assayed using the visible absorbance at 402 nm (ϵ = 102 mM^{-1} cm^{-1}) (24). The average milligrams/bead bed volume was 7.5 mg/ml. The quoted HRP activity is ~1300 units/mg based on the 2,2′-azino-bis-[3-ethylbenzthiazoline-6-sulfonic acid] (ABTS) assay. The resulting HRP_i activity/flat cell (100 μl) was 975 units or a concentration of 9750 units/ml. No attempt was made to evaluate the effect of immobilization on the enzyme activity.

Radical Generating Procedure Using HRP_i/H_2O_2/Tyrosine—L-Tyrosine (2 mM) or *N*-acetyl-L-tyrosine (4 mM) was dissolved in 50 mM phosphate buffer, pH 7.4, followed by the addition of H_2O_2 (1 mM). The tyrosine/H_2O_2 solution (50 ml) was then transferred to a 60-ml syringe and deaerated by purging with N_2 or argon gas for 20 min. When NO was used, the N_2 or argon purge was followed by purging the solution for 10 min with NO gas. The NO gas was initially passed through a scrubbing solution (10% KOH by weight) to remove contaminating higher oxides of nitrogen before bubbling through the tyrosine/H_2O_2 solutions. Before use, solutions were removed from the NO system and allowed to equilibrate to the desired 1.9 mM concentration. The solution was then flowed over HRP_i at 2 ml/min, and the ESR spectrum was recorded. Flow was controlled using a Harvard PHD 2000 syringe pump (Holliston, MA). The reaction mixture was in contact with the immobilized enzyme for ~2 s while passing through the sensitive region of the ESR spectrometer. For experimental consistency, all solutions were deaerated for 20 min prior to ESR data collection. When ascorbate was included in the reaction mixture, a small volume of ascorbic acid stock solution (deionized water, N_2-purged) was added to the deoxygenated tyrosine/H_2O_2 solution prior to the addition of NO.

Radical Generating Procedure Using HRP/H_2O_2/3-Nitroso-N-acetyl-L-tyrosine—The *N*-acetyl-L-tyrosine iminoxyl radical was generated by mixing free HRP (100 μg/ml), H_2O_2 (80 μM), and 3-nitroso-*N*-acetyl-L-tyrosine (~0.4 mM). This mixture was transferred to the ESR flat cell using an aspiration technique that allows ESR detection to be started within 10 s of initiating radical generation (25). The data presented in Fig. 4 used a phosphate buffer with 50% ethylene glycol to prevent aggregation upon freezing. Final buffer concentration was 50 mM, pH 7.8.

ESR Procedure/Analysis—ESR spectra (see Figs. 1–3) were collected at room temperature using a Bruker EMX spectrometer equipped with a SuperHigh Q cavity (Bruker Co., Billerica, MA) operated at 9.8 GHz with a 100-kHz modulation frequency. Spectrometer settings were 10-milliwatt microwave power, 1-G modulation amplitude, 164-ms time constant, 84-s scan time, and an average of nine scans over a 100-G scan range. ESR spectra (see Figs. 4 (*A*) and 5) were collected at room temperature using a Bruker Elexsys E 500 spectrometer equipped with an SHQ cavity (Bruker Co., Billerica, MA) operated at 9.8 GHz with a 100-kHz modulation frequency. Spectrometer settings were 10-milliwatt (Fig. 5) and 2-milliwatt (Fig. 4*A*) microwave power, 0.5-G (Fig. 5) and 1-G (Fig. 4*A*) modulation amplitude, 164-ms (Fig. 5) and 84-ms (Fig. 4*A*) time constant, 84-s (Fig. 5) and 42-s (Fig. 4*A*) scan time, and

[2] Sturgeon, B. E., Chen Y.-R., and Mason, R. P., manuscript in preparation.

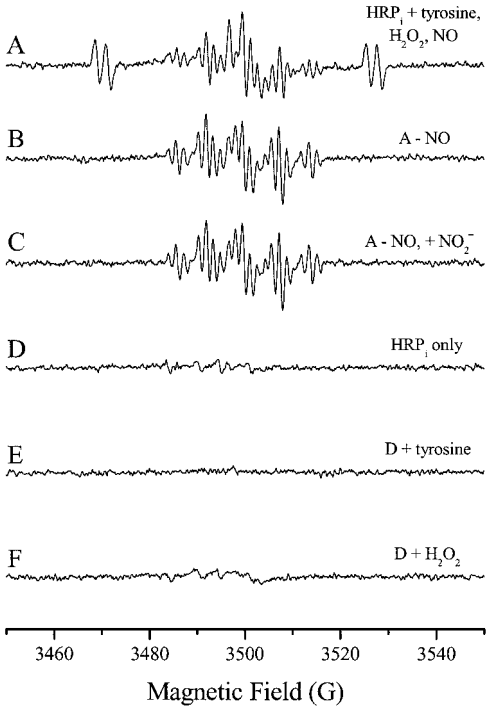

FIG. 1. **Direct ESR detection of the tyrosine iminoxyl radical.** The ESR spectrum detected when a solution of tyrosine (2 mM), H_2O_2 (1 mM), and NO (1.9 mM) was flowed over HRP$_i$ (*A*), a solution of tyrosine (2 mM) and H_2O_2 (1 mM) was flowed over HRP$_i$ (*B*), a solution of tyrosine (2 mM), H_2O_2 (1 mM), and NO_2^- (2 mM) was flowed over HRP$_i$ (*C*), buffer (50 mM phosphate) alone was flowed over HRP$_i$ (*D*), tyrosine (2 mM) alone was flowed over HRP$_i$ (*E*), and H_2O_2 (1 mM) alone was flowed over HRP$_i$ (*F*). ESR instrumental parameters were the same for all ESR spectra and are listed under "Experimental Procedures."

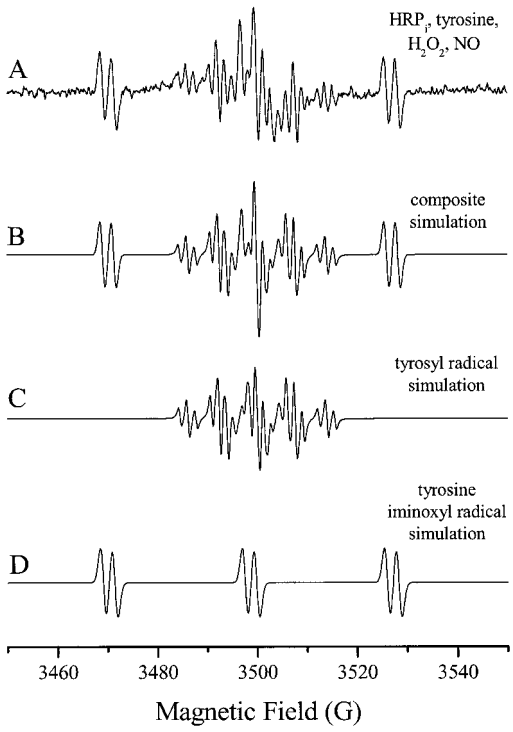

FIG. 2. **Simulation of the tyrosyl radical and the tyrosine iminoxyl radical.** *A*, the experimental ESR spectrum collected when a solution of tyrosine (2 mM), H_2O_2 (1 mM), and NO (1.9 mM) was flowed over HRP$_i$. *B*, the computer simulation of the composite spectrum in *panel A*. This composite spectrum was simulated using two species, the tyrosyl radical (75%) and the tyrosine iminoxyl radical (25%). *C*, the tyrosyl radical simulation using the hyperfine coupling constants $a^H_{3,5}$ = 6.35 G, $a^H_{2,6}$ = 1.60 G, a^H_β = 7.37 and 7.79 G, and the unresolved a^H_α = 0.28 G (27). *D*, the tyrosine iminoxyl radical simulation using the hyperfine coupling constants a^N = 28.4 G and a^H = 2.2 G.

an average of nine (Fig. 5) and 1 (Fig. 4*A*) scans over an 80-G (Fig. 5) and 100-G (Fig. 4*A*) scan range. The ESR spectrum in Fig. 4*B* was collected using a liquid nitrogen finger dewer on a Bruker Elexsys E 500 spectrometer. Spectrometer settings were 0.2-milliwatt microwave power, 2-G modulation amplitude, 328-ms time constant, 168-s scan time, and an average of 8 scans over a 200-G scan range. ESR simulations were carried out using the WINSIM program (Figs. 2 and 3) developed in our laboratory (26) and XSophe (Fig. 4) (Bruker Co.).

Absolute radical concentrations were measured against a 140 nM TEMPO standard (a stable nitroxide radical). Radical concentrations were measured by double integration of the ESR simulations of a given spectrum. The integration of the simulation provided numerical data that were unaffected by experimental baseline variations between data sets.

RESULTS

Direct ESR Detection of the Tyrosyl Radical and the Tyrosine Iminoxyl Radical—The ESR spectrum obtained when a deoxygenated solution of L-tyrosine (2 mM), H_2O_2 (1 mM), and NO (1.9 mM) was flowed over HRP$_i$ at 2 ml/min is shown in Fig. 1*A*. The ESR spectrum detected was a composite of two radical species that can be simulated using the known hyperfine coupling constants for the tyrosyl radical (27) and a radical species assigned as the tyrosine iminoxyl radical (a^N = 28.4 G and a^H = 2.2 G) (Fig. 2 and Scheme 1, *D*). The proton coupling of 2.2 G originated from tyrosine and was assigned to the proton *ortho* to the phenoxyl oxygen (see "Tyrosine Isotopic Substitution"). The assignment of the tyrosine iminoxyl radical was based on reported analogous iminoxyl radical hyperfine parameters (28, 29). As outlined in Scheme 1, the tyrosine iminoxyl radical is proposed to result from the secondary oxidation of 3-nitrosotyrosine (*C*) or the corresponding oxime (*C′*) formed from the reaction of the tyrosyl radical with NO. When NO was excluded from the reaction solution, only the tyrosyl radical was observed (Fig. 1*B*). It should be noted that NO is a good substrate for either HRP-I/II[3] (30) and that the product of this reaction is NO^+, which, at neutral pH values, is converted to nitrite. The addition of nitrite did not significantly affect the ESR spectrum (Fig. 1*C*) (31). Only a weak, unrelated ESR signal was detected with HRP$_i$ alone (Fig. 1*D*). The tyrosyl radical was a necessary precursor to the tyrosine iminoxyl radical (data not shown). The tyrosyl radical ESR signal requires H_2O_2 (Fig. 1*E*) and L-tyrosine (Fig. 1*F*).

Tyrosine Isotopic Substitution—The structure of the tyrosine iminoxyl radical shown as *D* in Scheme 1 is the most logical (18, 19); however, this structure has not been unequivocally assigned. Although NO can initially add to the tyrosyl radical at all positions of high spin density (Scheme 2), C-1 (0.37), C-2,6 (−0.06), C-3,5 (0.25), C-4 (−0.03), and $O_{phenoxyl}$ (0.25) (32–37), only addition to the C-3,5 positions can form the proposed iminoxyl radical. Isotopic labeling can be used to test this hypothesis.

Reference spectra, Fig. 3, *A–C*, present the tyrosyl radical spectrum (Fig. 3*A*), the composite spectrum containing the tyrosyl radical and the tyrosine iminoxyl radical (Fig. 3*B*), and the simulation of the composite spectrum (Fig. 3*C*). Note that

[3] HRP enzyme kinetics in the presence of NO are quite different in the absence of NO. When tyrosine is the only reducing substrate, HRP enzyme kinetics are determined by the relatively slow HRP-II oxidation of tyrosine. Because NO is a good substrate for both HRP-I and HRP-II, when NO is present, we are not under HRP-II limiting conditions, and the tyrosyl radical concentration is HRP-I-dependent but in competition with NO for HRP-I.

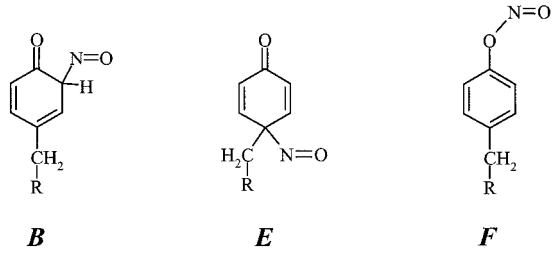

SCHEME 2.

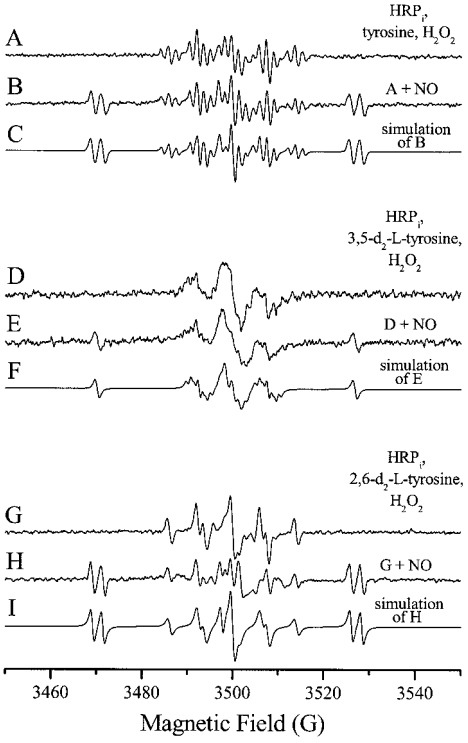

FIG. 3. **Direct ESR detection of the tyrosyl radical and the tyrosine iminoxyl radical using deuterated tyrosine isotopes.** The ESR spectrum collected when a solution of tyrosine (2 mM) and H_2O_2 (1 mM) was flowed over HRP_i (*A*) and a solution of tyrosine (2 mM), H_2O_2 (1 mM), and NO (1.9 mM) (*B*) was flowed over HRP_i. *C*, the simulation of *spectrum B* (see the legend for Fig. 2 for details). *D*, the ESR spectrum collected when a solution of 3,5-d_2-tyrosine (2 mM) and H_2O_2 (1 mM) was flowed over HRP_i. *E*, a solution of 3,5-d_2-tyrosine (2 mM), H_2O_2 (1 mM), and NO (1.9 mM) flowed over HRP_i. *F*, the simulation of *spectrum E* using the following parameters: 3,5-d_2-tyrosyl radical ($a^D_{3,5}$ = 0.97 G with all other simulation parameters unchanged) and the 3,5-d_2-tyrosine iminoxyl radical (a^N = 28.4 G). The ESR spectrum collected when a solution of 2,6-d_2-tyrosine (2 mM) and H_2O_2 (1 mM) was flowed over HRP_i (*G*) and a solution of 2,6-d_2-tyrosine (2 mM), H_2O_2 (1 mM), and NO (1.9 mM) was flowed over HRP_i (*H*) is shown. *I*, the simulation of *spectrum H* using the following parameters: 2,6-d_2-tyrosyl radical ($a^D_{2,6}$ = 0.25 G with all other simulation parameters unchanged) and the 2,6-d_2-tyrosine iminoxyl radical (a^N = 28.4 G and a^H = 2.2 G).

the tyrosine iminoxyl spectrum is characterized by a single nitrogen and a single proton coupling. Isotopic substitution of L-tyrosine with the 3,5-d_2-L-tyrosine (see Scheme 1 for atom numbering) resulted in the collapse of the small 2.2-G hyperfine coupling constant of the tyrosine iminoxyl radical (Fig. 3*E*). This observation confirms the identity of the 2.2-G proton coupling to be in the 5 position. In addition, the tyrosyl radical spectrum changed as predicted by the difference in the gyromagnetic ratio between protons and deuterons, thus confirming the original 3,5-d_2 isotopic substitution. Isotopic substitution of tyrosine with 2,6-d_2-L-tyrosine did not affect the tyrosine iminoxyl radical signal (Fig. 3*H*), although the tyrosyl radical ESR spectrum changed accordingly, again confirming the original 2,6-d_2 isotopic substitution.[4]

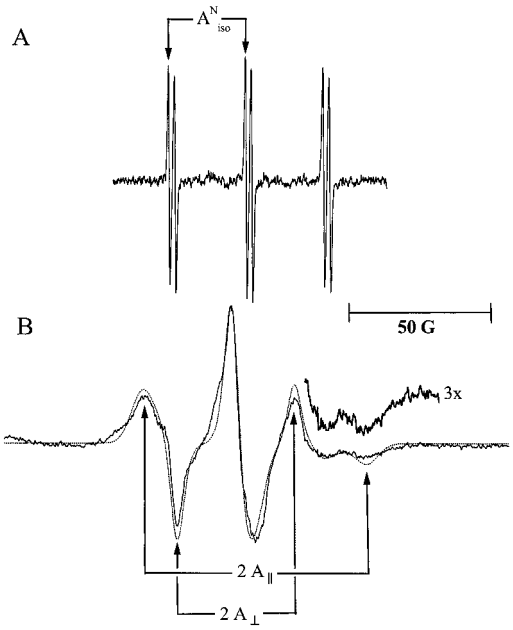

FIG. 4. **ESR detection of the tyrosine iminoxyl radical from 3-nitroso-*N*-acetyltyrosine.** *A*, the ESR spectrum collected 100 s after mixing HRP (100 μg/ml), H_2O_2 (80 μM), and 3-nitroso-*N*-acetyltyrosine (~0.4 mM) in a 50 mM phosphate buffer containing 50% ethylene glycol, pH 7.8. This mixture was aspirated into the ESR flat cell. *B*, the liquid nitrogen ESR spectrum collected from the same mixture in A, frozen 110 s after mixing. *Overlay*, computer simulation of *spectrum B*; see "Results" for g values, hyperfine couplings, and linewidths. ESR conditions are described under "Experimental Procedures."

HRP Oxidation of 3-Nitroso-N-acetyl-L-tyrosine—To further verify the assignment of the tyrosine iminoxyl radical, we synthesized 3-nitroso-*N*-acetyl-L-tyrosine (Scheme 1, *C*), a proposed intermediate in the HRP/H_2O_2/tyrosine/NO system. 3-Nitroso-*N*-acetyl-L-tyrosine was synthesized (as opposed to 3-nitroso-L-tyrosine) because the solubility of the starting material *N*-acetyl-L-tyrosine was considerably greater than L-tyrosine and also to prevent additional chemistry at the amine group of tyrosine. The oxidation of 3-nitroso-*N*-acetyl-L-tyrosine by HRP/H_2O_2 resulted in an ESR spectrum nearly identical to that detected in the HRP_i/H_2O_2/tyrosine/NO system, with hyperfine coupling constants a^N = 28.2 G and a^H = 2.2 G (Fig. 4*A*). The *N*-acetyl-L-tyrosine iminoxyl radical was formed in a 50% ethylene glycol-buffered solution; identical spectra were obtained in purely aqueous buffers (data not shown). At the time that the solution phase spectrum was collected, a portion of the reaction mixture was frozen in liquid nitrogen. The ESR spectrum collected at 77 K was that of an immobilized iminoxyl radical nearly identical to that observed in photosystem II (18) and prostaglandin H synthase-2 (19) systems (Fig. 4*B*). The ESR hyperfine coupling parameters measured from the immobilized ESR spectrum shown in Fig. 4*B* are $A_{\parallel}$ = 39.0 G and $A_{\parallel}$ = 20.8 G with $A_{iso} = (A_{\parallel} + 2A_{\perp})/3$ = 27.1 G. Computer simulation of this immobilized iminoxyl radical generated the following values: A_{xx} = 21.5 G, A_{yy} = 25.5 G, A_{zz} = 40.5 G, g_{xx} = 2.0064, g_{yy} = 2.0051, and g_{zz} = 2.0022, linewidths x = 2.4 G, y = 5.0 G, and z = 4.6 G. The ability to detect the *N*-acetyl-L-tyrosine iminoxyl radical depended markedly on the H_2O_2 concentration. The higher the H_2O_2 concentration, the larger the initial flux of iminoxyl radical, but the shorter the lifetime. This dependence on the H_2O_2 concentration implies that the

[4] The experimental spectrum of the 2,6-d_2-L-tyrosine/NO spectrum (Fig. 3*H*) appears to contain additional radical species not accounted for in the simulation (Fig. 3*I*).

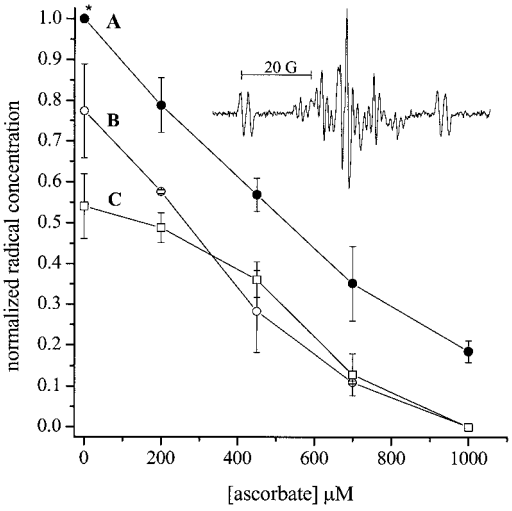

FIG. 5. **Tyrosine iminoxyl reactivity with ascorbate.** The direct ESR detection of the tyrosine iminoxyl radical was carried out in the presence of varying concentrations of ascorbate. *Trace A*, the effect of ascorbate on the concentration of the tyrosyl radical. *Trace B*, the effect of ascorbate on the concentration of the tyrosyl radical in the presence of NO. *Trace C*, the effect of ascorbate on the concentration of the tyrosine iminoxyl radical. The normalized radical concentration was based on the double integration of the tyrosyl radical spectrum. The data presented represent two sets of data that have been normalized to the *N*-acetyl-L-tyrosyl radical concentration in the absence of NO and ascorbate. The data point (*) representing the normalized concentration of *N*-acetyl-L-tyrosyl radical in the absence of ascorbate and NO was an actual concentration of 208 and 284 nM based on TEMPO standards. Substrate concentrations were *N*-acetyltyrosine (4 mM), H_2O_2 (1 mM), NO (1.9 mM), and ascorbate (ranged from 0 to 1000 μM). All solutions were made up in deoxygenated 100 mM phosphate buffer at pH 7.4. *Inset*, experimental ESR spectrum (ascorbate, 200 μM) showing all three radicals: tyrosyl radical, tyrosine iminoxyl radical, and ascorbate semidione radical.

iminoxyl radical is also a suitable HRP-I/II substrate presumably being oxidized to nitrotyrosine (18, 19).

Reactivity of the Tyrosyl Radical and the Tyrosine Iminoxyl Radical with the Antioxidant Ascorbate—The role of ascorbate to protect from free radical damage has received much attention. For this reason we investigated the reaction of the tyrosyl radical/tyrosine iminoxyl radical with the antioxidant ascorbate. The data shown in Fig. 5 used *N*-acetyl-L-tyrosine as opposed to L-tyrosine because background signals attributed to tyrosine oxidation products were much more prevalent in the case of L-tyrosine. The addition of ascorbate to the HRP_i/H_2O_2/*N*-acetyl-L-tyrosine system decreased the *N*-acetyl-L-tyrosyl radical signal as expected (Fig. 5, *trace A*) (38, 39). The addition of ascorbate to the HRP_i/H_2O_2/*N*-acetyl-L-tyrosine/NO system decreased both the *N*-acetyl-L-tyrosyl radical signal (Fig. 5, *trace B*) and the *N*-acetyl-L-tyrosine iminoxyl radical signal (Fig. 5, *trace C*). The rate of ascorbate reduction of the *N*-acetyl-L-tyrosyl radical was similar in the presence and absence of NO. The rate of ascorbate reduction of the *N*-acetyl-L-tyrosine iminoxyl radical appears to follow that of the *N*-acetyl-L-tyrosyl radical, indicating that ascorbate is reacting faster with the *N*-acetyl-L-tyrosyl radical than with the *N*-acetyl-L-tyrosine iminoxyl radical. It should be noted that ascorbate is a relatively poor substrate for HRP-I/II (40, 41).

DISCUSSION

Our results support the reaction mechanism for tyrosine iminoxyl radical formation shown in Scheme 1. We have confirmed the existence of the tyrosine iminoxyl radical, with structure *D* in Scheme 1, and that this iminoxyl radical is an enzymatic oxidation product from a solution containing tyrosine and NO. The synthesis and oxidation of 3-nitroso-*N*-acetyltyrosine provides additional support that 3-nitrosotyrosine (*C* in Scheme 1) is the intermediate in the pathway depicted in Scheme 1. In addition, the immobilized (77K) ESR spectrum of the *N*-acetyltyrosine iminoxyl radical has ESR parameters nearly identical to the iminoxyl radicals detected in photosystem II and prostaglandin H synthase-2, further supporting the formation of these intermediates in these enzyme systems.

In addition to the structural and mechanistic information, the reactivity of the tyrosine iminoxyl radical with the antioxidant ascorbate ($AscH^-$) has been shown to be primarily dependent on the concentration of the tyrosyl radical. The primary reactions involved are shown in Reaction Scheme 1.

$$\text{Tyrosyl radical} + AscH^- \rightarrow \text{tyrosine} + Asc^{\cdot-} \quad \text{(Eq. 1)}$$

$$\text{Tyrosyl radical} + NO \rightleftarrows \text{tyrosyl radical/NO weak complex } (B) \quad \text{(Eq. 2)}$$

$$\text{Tyrosyl radical/NO weak complex} \rightarrow \text{nitrosotyrosine } (C/C') \quad \text{(Eq. 3)}$$

$$\text{Nitrosotyrosine} \rightarrow \text{tyrosine iminoxyl radical } (D) \quad \text{(Eq. 4)}$$

$$\text{Tyrosyl radical/NO weak complex} \rightarrow \text{tyrosine iminoxyl radical} \quad \text{(Eq. 5)}$$

$$\text{Tyrosine iminoxyl radical} + Asc^- \rightarrow \text{nitrosotyrosine} + Asc^{\cdot-} \quad \text{(Eq. 6)}$$

REACTION SCHEME 1

Ascorbate and NO effectively compete for the tyrosyl radical, $k_1 = 4.4 \times 10^8\ M^{-1}\ s^{-1}$ (42) and $k_2 = 1 \times 10^9\ M^{-1}\ s^{-1}$ (21), respectively, although the reversible nature of the tyrosyl radical-NO weak complex (*Scheme 1*, *B*) formation (43–46) apparently results in more ascorbate quenching of the tyrosyl radical (Fig. 5). Note that 1 mM ascorbate quenches all tyrosyl radical and tyrosine iminoxyl radical (Fig. 5, *B* and *C*), but 1.9 mM NO quenches only ~20% of the tyrosyl radical (compare *trace A* with *trace B*). This situation is complicated by the change in enzyme kinetics in the presence of NO.[3]

The HRP_i/H_2O_2/tyrosine/NO system under investigation here clarifies a previous discussion about the formation of the tyrosyl radical-NO weak complex in the presence of additional oxidizing equivalents (18, 19). The reversible reaction of NO and tyrosyl radical can act to "buffer" the tyrosyl radical concentration (45). Since the HRP_i/H_2O_2 system described in this paper can provide oxidizing equivalents (as is the case with photosystem II and prostaglandin H synthase-2), the relatively slow reversible nature of the NO/tyrosyl radical reaction may be less important especially if the tyrosyl radical-NO weak complex can be directly oxidized to the tyrosine iminoxyl radical (Reaction Scheme 1, Eq. 5). The observation of the tyrosine iminoxyl radical from the HRP_i/H_2O_2/tyrosine/NO system allows us to make the following conclusion. The reaction between tyrosyl radical and NO forms oxidizable tyrosyl radical-NO intermediates (*B*, *C*, or *C′*); when these intermediates were formed in an oxidizing environment, one or more of them underwent a one-electron oxidation to form the tyrosine iminoxyl radical. Although nitrosotyrosine was not demonstrated to form as an intermediate, synthesized *N*-acetylnitrosotyrosine was facilely oxidized to the *N*-acetyltyrosine iminoxyl radical. It should be pointed out that the source of the oxidizing equivalence needed to form the tyrosine iminoxyl radical in the HRP_i/H_2O_2/tyrosine/NO system is HRP-I, HRP-II, or even the tyrosyl radical. Because the steady-state concentration of the tyrosyl radical is quite low, it is not expected to be the major source of oxidizing equivalents in our system. In non-enzymatic radical generating systems, the tyrosyl radical may be the only source of oxidizing equivalents, and thus the formation of the iminoxyl radical would be expected to be significantly less than in an enzymatic system (46).

Acknowledgments—We thank Jean Corbett and Dr. Yang Fann of NIEHS, National Institutes of Health, Laboratory of Pharmacology and Chemistry, for assistance in performing these studies and Dr. Carol E. Parker of NIEHS, National Institutes of Health, Laboratory of Structural Biology, for collecting the mass spectrometry data on 3-nitroso-*N*-acetyltyrosine.

REFERENCES

1. Stubbe, J., and van der Donk, W. A. (1998) *Chem. Rev.* **98,** 705–762
2. Barry, B. A., and Babcock, G. T. (1987) *Proc. Natl. Acad. Sci. U. S. A.* **84,** 7099–7103
3. Barry, B. A., El-Deeb, M. K., Sandusky, P. O., and Babcock, G. T. (1990) *J. Biol. Chem.* **265,** 20139–20143
4. Sjoberg, B. M., Reichard, P., Graslund, A., and Ehrenberg, A. (1977) *J. Biol. Chem.* **252,** 536–541
5. Sjoberg, B. M., Reichard, P., Graslund, A., and Ehrenberg, A. (1978) *J. Biol. Chem.* **253,** 6863–6865
6. Karthein, R., Dietz, R., Nastainczyk, W., and Ruf, H. H. (1988) *Eur. J. Biochem.* **171,** 313–320
7. Aubert, C., Brettel, K., Mathis, P., Eker, A. P. M., and Boussac, A. (1999) *J. Am. Chem. Soc.* **121,** 8659–8660
8. Aubert, C., Mathis, P., Eker, A. P. M., and Brettel, K. (1999) *Proc. Natl. Acad. Sci. U. S. A.* **96,** 5423–5427
9. Ivancich, A., Jouve, H. M., and Gaillard, J. (1996) *J. Am. Chem. Soc.* **118,** 12852–12853
10. Whittaker, M. M., and Whittaker, J. W. (1990) *J. Biol. Chem.* **265,** 9610–9613
11. Babcock, G. T., El-Deeb, M. K., Sandusky, P. O., Whittaker, M. M., and Whittaker, J. W. (1992) *J. Am. Chem. Soc.* **114,** 3727–3734
12. MacMillan, F., Kannt, A., Behr, J., Prisner, T., and Michel, H. (1999) *Biochemistry* **38,** 9179–9184
13. Petrouleas, V., and Diner, B. A. (1990) *Biochim. Biophys. Acta* **1015,** 131–140
14. Szalai, V. A., and Brudvig, G. W. (1996) *Biochemistry* **35,** 15080–15087
15. Lepoivre, M., Fieschi, F., Coves, J., Thelander, L., and Fontecave, M. (1991) *Biochem. Biophys. Res. Commun.* **179,** 442–448
16. Lepoivre, M., Chenais, B., Yapo, A., Lemaire, G., Thelander, L., and Tenu, J. P. (1990) *J. Biol. Chem.* **265,** 14143–14149
17. Lepoivre, M., Flaman, J. M., Bobe, P., Lemaire, G., and Henry, Y. (1994) *J. Biol. Chem.* **269,** 21891–21897
18. Sanakis, Y., Goussias, C., Mason, R. P., and Petrouleas, V. (1997) *Biochemistry* **36,** 1411–1417
19. Gunther, M. R., Hsi, L. C., Curtis, J. F., Gierse, J. K., Marnett, L. J., Eling, T. E., and Mason, R. P. (1997) *J. Biol. Chem.* **272,** 17086–17090
20. Goodwin, D. C., Gunther, M. R., Hsi, L. C., Crews, B. C., Eling, T. E., Mason, R. P., and Marnett, L. J. (1998) *J. Biol. Chem.* **273,** 8903–8909
21. Eiserich, J. P., Butler, J., Van der Vliet, A., Cross, C. E., and Halliwell, B. (1995) *Biochem. J.* **310,** 745–749
22. Beckman, J. S., Wink, D. A., and Crow, J. P. (1996) in *Methods in Nitric Oxide Research* (Feelisch, M., and Stamler, J. S., eds) pp. 61–70, John Wiley & Sons, New York
23. Maruyama, K., Tanimoto, I., and Goto, R. (1967) *J. Org. Chem.* **32,** 2516–2520
24. Schonbaum, G. R., and Lo, S. (1972) *J. Biol. Chem.* **247,** 3353–3360
25. Mason, R. P. (1984) *Methods Enzymol.* **105,** 416–422
26. Duling, D. R. (1994) *J. Magn. Reson. Ser. B* **104,** 105–110
27. Sealy, R. C., Harman, L., West, P. R., and Mason, R. P. (1985) *J. Am. Chem. Soc.* **107,** 3401–3406
28. Thomas, J. R. (1964) *J. Am. Chem. Soc.* **86,** 1446–1447
29. Green, R. G., Sutcliffe, L. H., and Preston, P. N. (1975) *J. Chem. Soc. Perkin Trans. II* 1380–1384
30. Glover, R. E., Koshkin, V., Dunford, H. B., and Mason, R. P. (1999) *Nitric Oxide: Biol. Chem.* **3,** 439–444
31. Roman, R., and Dunford, H. B. (1973) *Can. J. Chem.* **51,** 588–596
32. Dole, F., Diner, B. A., Hoganson, C. W., Babcock, G. T., and Britt, R. D. (1997) *J. Am. Chem. Soc.* **119,** 11540–11541
33. Warncke, K., Babcock, G. T., and McCracken, J. (1994) *J. Am. Chem. Soc.* **116,** 7332–7340
34. Hoganson, C. W., and Babcock, G. T. (1992) *Biochemistry* **31,** 11874–11880
35. Bender, C. J., Sahlin, M., Babcock, G. T., Barry, B. A., Chandrashekar, T. K., Salowe, S. P., Stubbe, J., Lindstrom, B., Petersson, L., Ehrenberg, A., and Sjoberg, B. M. (1989) *J. Am. Chem. Soc.* **111,** 8076–8083
36. Rigby, S. E. J., Nugent, J. H. A., and O'Malley, P. J. (1994) *Biochemistry* **33,** 1734–1742
37. Tommos, C., Tang, X. S., Warncke, K., Hoganson, C. W., Styring, S., McCracken, J., Diner, B. A., and Babcock, G. T. (1995) *J. Am. Chem. Soc.* **117,** 10325–10335
38. Rao, D. N. R., Fischer, V., and Mason, R. P. (1990) *J. Biol. Chem.* **265,** 844–847
39. Sturgeon, B. E., Sipe, H. J., Barr, D. P., Corbett, J. T., Martinez, J. G., and Mason, R. P. (1998) *J. Biol. Chem.* **273,** 30116–30121
40. Yamazaki, I., and Piette, L. H. (1961) *Biochim. Biophys. Acta* **50,** 62–69
41. Yamazaki, I. (1977) in *Free Radicals in Biology* (Pryor, W. A., ed) Vol. III, pp. 183–218, Academic Press, New York
42. Hunter, E. P. L., Desrosiers, M. F., and Simic, M. G. (1989) *Free Radic. Biol. Med.* **6,** 581–585
43. Yu, T., Mebel, A. M., and Lin, M. C. (1995) *J. Phys. Org. Chem.* **8,** 47–53
44. Berho, F., Caralp, F., Rayez, M. T., Lesclaux, R., and Ratajczak, E. (1998) *J. Phys. Chem. A* **102,** 1–8
45. Stanbro, W. D. (1999) *J. Theor. Biol.* **197,** 557–567
46. Goldstein, S., Czapski, G., Lind, J., and Merenyi, G. (2000) *J. Biol. Chem.* **275,** 3031–3036

Tyrosine Iminoxyl Radical Formation from Tyrosyl Radical/Nitric Oxide and Nitrosotyrosine

Bradley E. Sturgeon, Richard E. Glover, Yeong-Renn Chen, Leo T. Burka and Ronald P. Mason

J. Biol. Chem. 2001, 276:45516-45521.
doi: 10.1074/jbc.M106835200 originally published online September 10, 2001
